Pergamon

Int. J. Heat Mass Transfer. Vol. 38, No. 7, pp. 1217–1224, 1995

0017-9310/95 $9.50+0.00

0017-9310(94)00243-6

Local particle convective heat transfer along surfaces in circulating fluidized beds

Z. H. FANG,† J. R. GRACE‡ and C. J. LIM

Department of Chemical Engineering, University of British Columbia, Vancouver, Canada V6T 1Z4

(*Received* 4 *March* 1994 *and in final form* 22 *July* 1994)

Abstract—The relationship between heat dissipation of individual clusters and local heat transfer to a surface in a circulating fluidized bed has been established based on a probabilistic cluster renewal model. Variations of local particle convective heat transfer coefficient with length are predicted based on the model. A simplified model assuming an identical contact distance of clusters leads to explicit expressions for the local and average particle convective heat transfer coefficients, which approximate the more rigorous model for most cases of practical interest. Previous experimental data for heat transfer to a membrane wall are in good agreement with model predictions. Information on the wall contact resistance and mean cluster contact distance is also obtained from the model in combination with the experimental data.

INTRODUCTION

Compared to the long history of the traditional bubbling fluidization, circulating fluidized beds (CFB) are a recent development. Considerable efforts have been made to understand and predict the performance of heat transfer between a circulating fluidized bed and a fixed surface as reviewed by Grace [1, 2]. This kind of heat transfer is quite complicated, and usually considered to consist of convective and radiative components. In most models proposed by various researchers the convective transfer of the dense phase has been based on transient conduction from the solid aggregates (clusters), a model inherited from the packet theory for bubbling fluidized bed heat transfer. The theory was originally proposed by Mickley and Fairbanks [3], who derived an expression for the transient convective component of the solid packet as

$$h_{t1}(t) = \sqrt{\frac{k_e \rho c}{\pi t}}. \tag{1}$$

By integrating equation (1) over time, a time-averaged coefficient of this component can be obtained

$$\overline{h_{t1}}(t) = 2 \cdot h_{t1}(t). \tag{2}$$

The theory was improved later by Baskakov [4] to incorporate a thermal contact resistance, R_w, between the solid packet and wall into the model, which led to following transient and averaged heat transfer coefficients from the packets

$$h_{t2}(t) = \frac{1}{R_w} \exp\left(\frac{t}{R_w^2 k_e \rho c}\right) \operatorname{erfc}\left(\frac{1}{R_w}\sqrt{\frac{t}{k_e \rho c}}\right) \tag{3}$$

$$\overline{h_{t2}}(t) = \frac{R_w k_e \rho c}{t}\left[\exp\left(\frac{t}{R_w^2 k_e \rho c}\right) \operatorname{erfc}\left(\frac{1}{R_w}\sqrt{\frac{t}{k_e \rho c}}\right) + \frac{2}{\sqrt{\pi} R_w}\sqrt{\frac{t}{k_e \rho c}} - 1\right]. \tag{4}$$

These expressions are somewhat inconvenient for engineering calculations due to the presence of the complementary error function term. Utilizing the concept of resistances in series, equations (3) and (4) are often approximated by

$$h_{t3} = \frac{1}{R_w + \sqrt{\frac{\pi t}{k_e \rho c}}} \tag{5}$$

$$\overline{h_{t3}} = \frac{1}{R_w + \sqrt{\frac{\pi t}{4 k_e \rho c}}} \tag{6}$$

with the worst deviations from the analytical solution of equations (3) and (4) being about -16% for equation (5) and -4.8% for equation (6), respectively. Other relations for packet transient conduction with various boundary conditions have been summarized by Gelperin and Einstein [5]. Recent experimental evidence [6] has shown that packet-type transient decay models describe only part of traces of local instantaneous heat transfer to horizontal tubes in bubbling fluidized beds.

In both commercial and laboratory CFB units there exists a core–annulus structure, where solid particles are carried upward in a dilute central core and congregate to form clusters or streamers and descend in a much denser annulus layer near the containing wall of the riser. As they slide downward along the wall, the clusters may maintain contact with the wall for a

† On leave from Shandong Institute of Civil Engineering, Jinan, P. R. China 250014.

‡ Author to whom correspondence should be addressed.

NOMENCLATURE

c	specific heat of clusters
d_p	mean particle diameter
h	heat transfer coefficient
k_e	effective thermal conductivity of clusters
k_g	thermal conductivity of gas
K	dimensionless parameter, given by equation (13)
L	mean contact distance of clusters
l	distance cluster has been in contact with the heat transfer surface
n	parameter in gamma distribution, given by equation (7)
Nu	$h \cdot R_w$, Nusselt number
p	density function of probability distribution
R_w	thermal contact resistance
s	contact distance of clusters
S	survival function, given by equation (9)
t	time
u	descending velocity of clusters
x	coordinate
x'	height at which cluster first makes contact with the wall
x_0	length of adiabatic section of wall
X	x/L, dimensionless coordinate
X_0	x_0/L, dimensionless parameter
z	$x-x'$, integration variable.

Greek symbols

δ	ratio of gas gap width to particle diameter
θ	parameter in gamma distribution, given by equation (7)
ρ	density of clusters
σ	standard deviation of probability distribution.

Subscripts and superscript

t	transient model
x	local model
$\bar{}$	averaged.

limited period of time, and then either drift away from the wall or disintegrate. When there is a heat transfer surface on the wall, the clusters contacting it undergo transient conduction and exchange heat with the wall. While the analogy between the bubbling bed and CFB has been helpful, heat transfer to outer vertical walls in circulating (fast-fluidized) beds differs significantly from that to immersed tubes in bubbling beds. One feature reported by various researchers, e.g. Wu *et al.* [7], is the significant effect of the length of heat transfer surfaces. This can be explained qualitatively by equations (1) and (3), because a longer heat transfer surface tends to mean a longer contact time of the clusters. If, for simplicity, it is assumed that all clusters descend at a constant speed, u, a rational approach to this problem is to take the time for the clusters to slide along the surface height as the contact time, or for surfaces which are long enough that renewal is expected on them, to assume a characteristic residence length and take the time for clusters to traverse this distance as the contact time in evaluating their convective heat transfer. Glicksman [8] proposed a model in which a sheet of particles was assumed to accelerate from rest to a maximum velocity so that the contact time could be estimated.

All these models of cluster convective heat transfer trace the movement and thermal history of individual clusters, rather than considering fixed locations. Therefore they are transient heat transfer models rather than 'local' ones. While they can predict the general trend and the right limits of heat transfer coefficient for very short and very long surfaces, these models fail to reveal an accurate picture of the variation of local heat transfer coefficient with length. The model proposed by Wu *et al.* [9] tried to take this effect into account on an analytical basis. In this model the clusters were supposed to contact the surface at its top level and, after traveling a characteristic distance, to mix with other particles in an outer annular layer and reform. Although this model indicates the general trend of the surface length effect and gives reasonable order-of-magnitude estimates of the heat transfer coefficient for representative measured results after its parameters have been fitted using experimental data, the non-monotonic and non-smooth variation of the heat transfer coefficient with length resulting from the assumption of stage-by-stage mixing is unrealistic. In this paper we seek an improved heat transfer model where clusters reach the wall at different positions and travel different distances. While this representation is not expected to be perfect, it provides a more realistic basis for prediction than previous models.

LOCAL TRANSFER MODEL

Here we present a model for particle convective heat transfer. The contributions of radiation and gas convection can usually be treated separately as additive components [2, 10]. For the particle convective transfer the following assumptions are adopted.

1. The circulating fluidized bed is contained in a riser with a continuous wall consisting of an isothermal heat transfer surface, with an adiabatic one

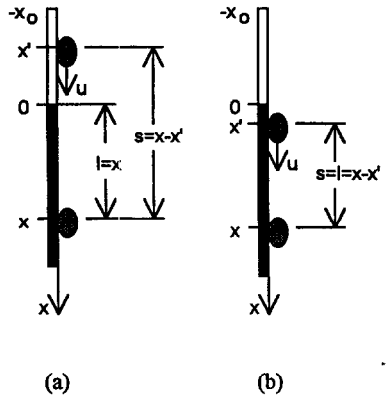

Fig. 1. Heat transfer configuration for (a) cluster contacting wall above the heat transfer surface and (b) cluster contacting the wall at some distance below the top of the heat transfer surface.

above it of height x_0 as shown in Fig. 1. The coordinate origin is located at the top of the heat transfer surface. The specific case $x_0 = 0$ corresponds to absence of the adiabatic section of the wall.

2. The clusters make contact with the wall evenly throughout both wall sections, with a uniform probability of arrival at any height. Once clusters reach the wall, they descend along the wall at a constant velocity, u. The transient heat transfer coefficient of each cluster can be expressed as a function of its contact time, $h_t(t)$, given by equation (3).

3. The contact lifetime and contact distance, s, of individual clusters from their initial contact with the wall to their disintegration or inward migration is random, conforming to a probability distribution with a density function $p(s)$. Having been found useful in describing a wide range of lifetime probabilities, a gamma distribution is adopted as a first approximation. The gamma distribution has a density function

$$\left.\begin{aligned} p(s) &= \frac{\theta^n s^{n-1} e^{-\theta s}}{\Gamma(n)} \quad \text{if} \quad s \geqslant 0 \\ p(s) &= 0, \qquad\qquad\quad \text{if} \quad s < 0 \end{aligned}\right\} \tag{7}$$

with both parameters θ and n greater than zero, and

$$\Gamma(n) = \int_0^\infty s^{n-1} e^{-s}\, ds. \tag{8}$$

For an integer n, equation (8) reduces to $\Gamma(n) = (n-1)!$

The gamma distribution given by equation (7) has a mean of $L = n/\theta$ and variance of $\sigma^2 = n/\theta^2$. In the special case of $n = 1$ the gamma distribution reduces to an exponential distribution, which is less suitable for this situation. In the absence of knowledge of the parameter n based on experiments, we can only estimate $n \geqslant 2$ at present.

The 'survival function' $S(z)$ of a certain density $p(s)$, defined as

$$S(z) = \int_z^\infty p(s)\, ds = 1 - \int_0^z p(s)\, ds \tag{9}$$

indicates the probability for the clusters to survive after traveling a distance z along the wall. In the case of gamma distribution with $n \geqslant 2$, the survival function will be less than 0.01 for $z/L > 1 + 3.5/\sqrt{n}$. This means that there is little chance that a cluster will traverse a distance, say, of three times the mean distance for $n \geqslant 2$.

Heat is transferred to a certain differential area located at x by various clusters with different contact and conduction experiences. Suppose a cluster starts its contact with the wall at x'. The probability for it to pass the area of interest at x is given by

$$P = \int_{x-x'}^\infty p(s)\, ds. \tag{10}$$

When this cluster reaches the area of interest, it has traversed a heat transfer distance of $l = x$ for $x' \leqslant 0$, or $l = x - x'$ for $x' > 0$. Heat is then transferred with an instantaneous coefficient $h_t(x/u)$ or $h_t[(x-x')/u]$ as described by the transient model. The local heat transfer coefficient $h_x(x)$ is determined by averaging contributions of all these clusters, weighted with their contact probability, i.e.

$$h_x(x) = \frac{\displaystyle\int_{-x_0}^0 h_t\left(\frac{x}{u}\right)\int_{x-x'}^\infty p(s)\, ds\, dx' + \int_0^x h_t\left(\frac{x-x'}{u}\right)\int_{x-x'}^\infty p(s)\, ds\, dx'}{\displaystyle\int_{-x_0}^x \int_{x-x'}^\infty p(s)\, ds\, dx'}. \tag{11}$$

Substituting equations (3) and (7) into equation (11), we can see that the local heat transfer coefficient is a function of the location x, as well as other parameters, i.e.

$$h_x = f(x, x_0, u, R_w, k_e, \rho c, \theta, n). \tag{12}$$

The wall contact resistance R_w depends mainly on the particle size, while the effective thermal properties k_e, ρ and c are functions of cluster voidage. These variables are expected to play important roles in determining the heat transfer performance. The cluster lifetime distribution parameters θ and n likely depend upon geometric configuration and hydrodynamic conditions.

The parameter $\theta = n/L$ has units of reciprocal length. Alternatively, use of the expected contact distance, or the mean of the distribution, L, as an independent parameter is more convenient in engineering

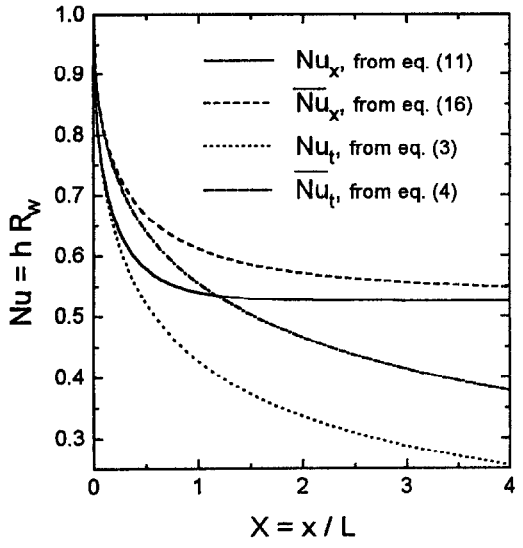

Fig. 2. Heat transfer coefficients predicted by transient and local models for $n = 2$, $K = 1$, $X_0 = 3$.

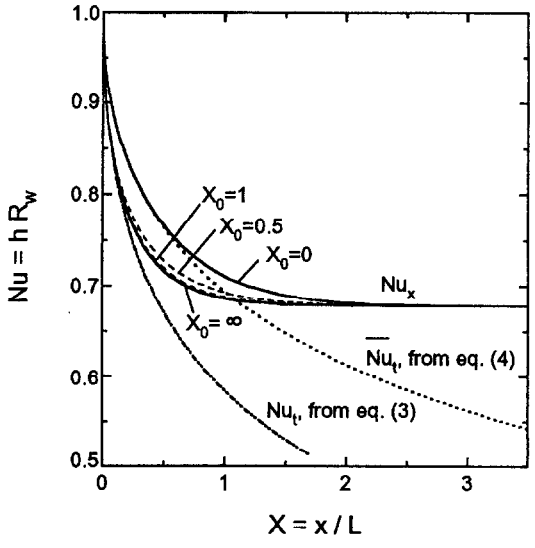

Fig. 3. The effect of x_0 on the local heat transfer coefficient for $n = 4$, $K = 1$.

applications. With L as a characteristic length we define dimensionless parameters

$$\left.\begin{aligned} X &= x/L \\ X_0 &= x_0/L \\ Nu &= h \cdot R_w \\ K &= \frac{1}{R_w}\sqrt{\frac{L}{k_e \rho c u}} \end{aligned}\right\}. \tag{13}$$

K is the ratio of the characteristic conductive resistance inside the cluster to the contact resistance on the wall. Nu is a special Nusselt number with limits between 0 and 1. This definition helps to reduce the number of dimensionless parameters. Equation (12) can now be reformulated as a dimensionless expression

$$Nu_x = F(X, X_0, K, n). \tag{14}$$

The average heat transfer coefficient over a surface from 0 to x can be obtained by

$$\overline{h_x} = \frac{1}{x}\int_0^x h_x \, dx \tag{15}$$

or

$$\overline{Nu_x} = \frac{1}{X}\int_0^X Nu_x \, dX. \tag{16}$$

DISCUSSION

Figure 2 shows typical local and average particle convective heat transfer coefficients predicted by the transient model, i.e. equations (3) and (4), and this model. It can be seen that the heat transfer coefficients obtained by this model are greater than those from the transient model except for $x = 0$, where both models give $Nu = 1$. The difference can be accounted for by the fact that not all the clusters come into contact with the surface at its very top; instead there is continual renewal of the clusters reaching the wall. Moreover, while the transient theory predicts that cluster convective transfer diminishes to zero as the surface extends to infinity, according to the present model both the local and average heat transfer coefficients approach a constant value with increasing surface length. This is clearly more realistic.

Influence of the adiabatic section length x_0

As mentioned above, few clusters travel along the wall an unusually long distance, say, three or more times the mean distance. Therefore local heat transfer is hardly influenced by clusters which achieve contact with the wall high above the location under consideration. Some asymptotic limits of heat transfer can therefore be derived.

The heat transfer coefficient for long surfaces in CFB units is of great importance for industrial applications. For $x \gg L$, both local and average heat transfer coefficients approach the same limit, which is independent of x_0. On the other hand, x_0 does have a certain influence for short surfaces whose lengths are less than, or of the same order as, the cluster mean contact distance. Computation has also shown that increasing the length of adiabatic sections beyond three times the mean contact distance causes negligible change in heat transfer to the surface; in this case x_0 can be simply regarded as infinity. These features of the effects of x_0 are shown in Fig. 3. In most practical cases for short surfaces, such as small heat transfer probes installed in an insulated wall, there are large adiabatic areas around them. Then only the extreme of $x_0 = \infty$ is of practical importance. For many pur-

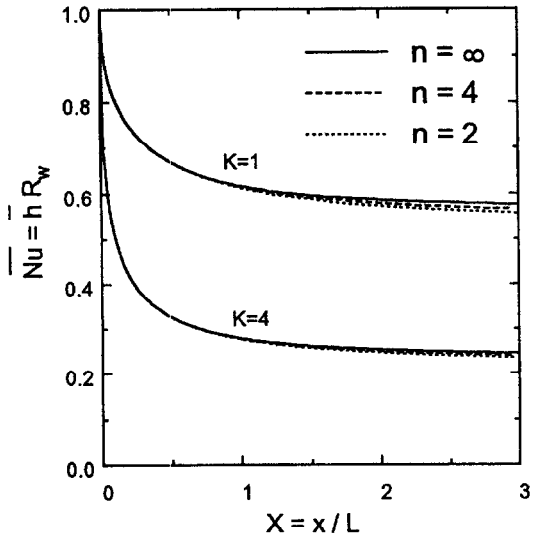

Fig. 4. Effect of n on the average heat transfer coefficient for $X_0 = 3$ and two values of K.

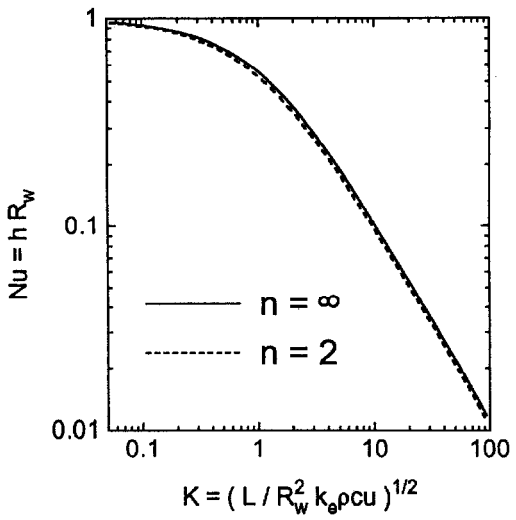

Fig. 5. Cluster convective heat transfer for very long surfaces ($X \gg 1$).

poses, the influence of x_0 can therefore be simplified by focusing on the two extremes, $x_0 = \infty$ and $x_0 = 0$.

Influence of contact distance variance

For the gamma distribution we have

$$\frac{\sigma}{L} = \frac{1}{\sqrt{n}} \tag{17}$$

so that the parameter n is related to the variance. The larger the parameter n, the more closely the cluster contact distances converge in a relative sense around their mean. The extreme of n approaching infinity turns the probabilistic distribution of the contact distances into a determinate one, which means that all clusters contact the wall for an identical distance, L. Average heat transfer coefficients are plotted in Fig. 4 for different values of n. They indicate, fortunately, that the parameter n has very little influence for $x < L/2$, and only a minor influence on the particle convective transfer for $x > L/2$. The greatest relative difference occurs for large X, and results for this case are plotted in Fig. 5. Computation has shown that the maximum difference between the heat transfer coefficients is only 7% for the two extremes $n = 2$ and $n = \infty$, with $n = \infty$ resulting in the highest rate. The minor significance of n can be accounted for by the fact that, when the contact distances diverge from their mean, the decrease in transfer from clusters traveling longer distances is partially offset by the gains from those traveling shorter distances. The minor influence of n indicates that the distribution of the contact distances is of secondary importance to the heat transfer. Due to lack of reliable information on the distribution of the contact distances, the following discussion focuses on the special case of determinate contact distance, i.e. $n = \infty$. Simpler approximations of the previous model can then be derived.

Determinate contact distance model

We consider here only the influence of the mean of the cluster contact distances, while restricting their variance to zero. As discussed above, the influence of the variance is of secondary importance. Hence this simplified model can be of practical value for general situations with a contact distance distribution. When the probabilistic model reduces to the determinate one, i.e. for $n = \infty$, we have

$$\left.\begin{aligned} \int_0^x p(s)\,\mathrm{d}s &= 0, \quad \text{for } x < L \\ \int_0^x p(s)\,\mathrm{d}s &= 1, \quad \text{for } x \geqslant L \end{aligned}\right\}. \tag{18}$$

Then, with a coordinate transformation $z = x - x'$ and with $X_0 \geqslant 1$, equation (11) reduces to

$$h_x(x) = \frac{1}{L}\left[h_t\left(\frac{x}{u}\right)\cdot(L-x) + \int_0^x h_t\left(\frac{z}{u}\right)\mathrm{d}z\right]$$

$$= \left(1-\frac{x}{L}\right)\cdot h_t\left(\frac{x}{u}\right) + \frac{x}{L}\cdot \bar{h}_t\left(\frac{x}{u}\right), \quad \text{for } x < L \tag{19}$$

$$h_x(x) = \frac{1}{L}\int_0^L h_t\left(\frac{z}{u}\right)\mathrm{d}z$$

$$= \bar{h}_t\left(\frac{L}{u}\right), \quad \text{for } x \geqslant L. \tag{20}$$

h_t and $\bar{h}_t$ can be obtained from any appropriate packet transient conduction model, e.g. equations (3) and (4). For the initial section with $x < L$, the local heat transfer is affected by two kinds of clusters. Clusters coming into contact above the heat transfer surface experience an identical instantaneous rate of $h_t(x/u)$, while those making contact with the wall within the

transfer section have different rates of transfer at this location. The average effect of the latter is just like the time-averaged heat transfer coefficient of a single cluster traveling from the top of the surface down to this location. Beyond this initial section, i.e. for $x \geqslant L$, the cluster renewal reaches dynamic equilibrium. The local heat transfer coefficient then becomes independent of the length coordinate. In this situation the local heat transfer coefficient is equal to $\bar{h}_t(L/u)$ instead of $h_t(L/u)$.

For $x_0 = 0$ the local heat transfer coefficient is further simplified to

$$h_x = \bar{h}_t\left(\frac{x}{u}\right), \quad \text{for } x < L; \tag{21}$$

$$h_x = \bar{h}_t\left(\frac{L}{u}\right), \quad \text{for } x \geqslant L. \tag{22}$$

Substituting equations (3) and (4) into the above expressions and making them dimensionless, we obtain

$$Nu_x = (1-X)\exp(K^2X)\cdot\operatorname{erfc}(K\sqrt{X}) + \frac{1}{K^2}\left[\exp(K^2X)\cdot\operatorname{erfc}(K\sqrt{X}) + \frac{2}{\sqrt{\pi}}K\sqrt{X} - 1\right] \quad \text{for } X_0 \geqslant 1,\ X < 1 \tag{23}$$

$$Nu_x = \frac{1}{K^2X}\left[\exp(K^2X)\cdot\operatorname{erfc}(K\sqrt{X}) + \frac{2}{\sqrt{\pi}}K\sqrt{X} - 1\right], \quad \text{for } X_0 = 0,\ X < 1 \tag{24}$$

$$Nu_x = \frac{1}{K^2}\left[\exp(K^2)\cdot\operatorname{erfc}(K) + \frac{2}{\sqrt{\pi}}K - 1\right], \quad \text{for } X \geqslant 1. \tag{25}$$

Of greater importance in applications, the length-averaged heat transfer coefficient can be obtained according to equation (16)

$$\overline{Nu}_x = \frac{1}{K^4X}\left[\exp(K^2X)\cdot\operatorname{erfc}(K\sqrt{X})\cdot(2+K^2-K^2X) - K^2 - 2 + \frac{2}{\sqrt{\pi}}K\sqrt{X}\left(\frac{1}{3}K^2X + K^2 - \frac{\sqrt{\pi}}{2}K\sqrt{X} + 2\right)\right], \quad \text{for } X_0 \geqslant 1,\ X < 1 \tag{26}$$

$$\overline{Nu}_x = \frac{1}{K^4X}\left[\exp(K^2)\cdot\operatorname{erfc}(K)\cdot(2-K^2) + \frac{2}{3\sqrt{\pi}}K^3 - K^2 + \frac{4}{\sqrt{\pi}}K - 2\right] + \frac{1}{K^2}\left[\exp(K^2)\cdot\operatorname{erfc}(K) + \frac{2}{\sqrt{\pi}}K - 1\right], \quad \text{for } X_0 \geqslant 1,\ X \geqslant 1. \tag{27}$$

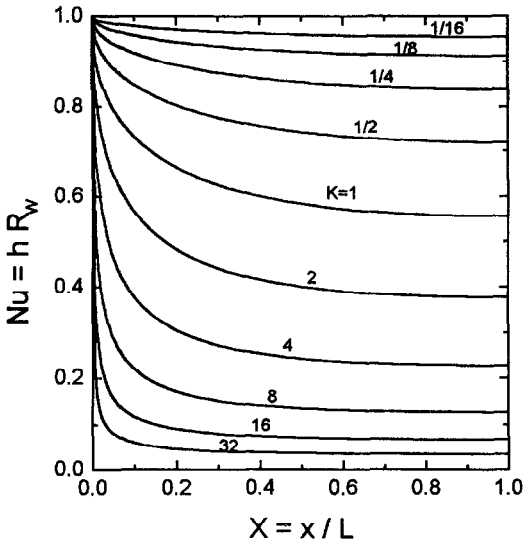

Fig. 6. Local heat transfer coefficient according to the determinate contact distance model for $X_0 \geqslant 1$.

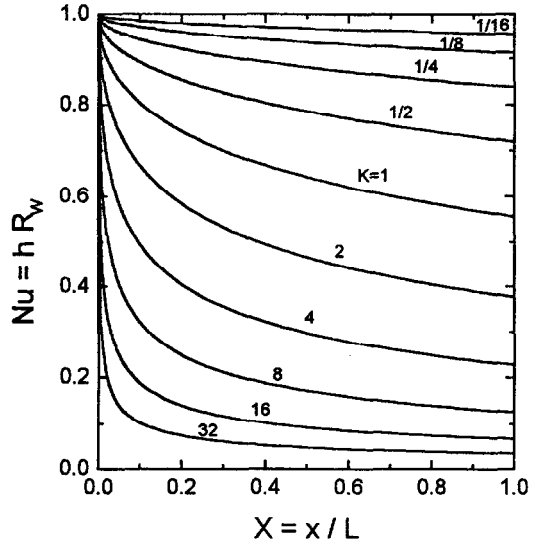

Fig. 7. Local heat transfer coefficient according to the determinate contact distance model for $X_0 = 0$.

It can be seen that the dimensionless heat transfer coefficient $Nu_x = h_x \cdot R_w$ turns out to be a function of three dimensionless parameters, i.e. X, X_0 and K. For $X_0 \geqslant 1$, the local and averaged Nusselt number is determined only by X and K. From its definition we know that K, the ratio of the characteristic conductive resistance inside the cluster to the contact resistance on the wall, represents the combined effects of R_w, L and the thermophysical properties of the cluster. Computed results are plotted in Figs. 6–8 for different values of K.

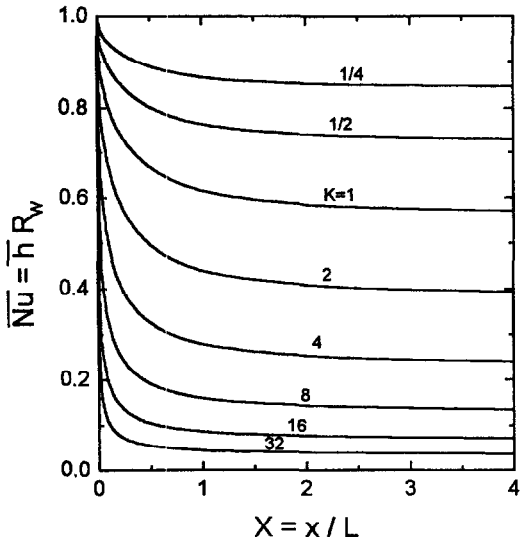

Fig. 8. Average heat transfer coefficient according to the determinate contact distance model for $X_0 \geqslant 1$.

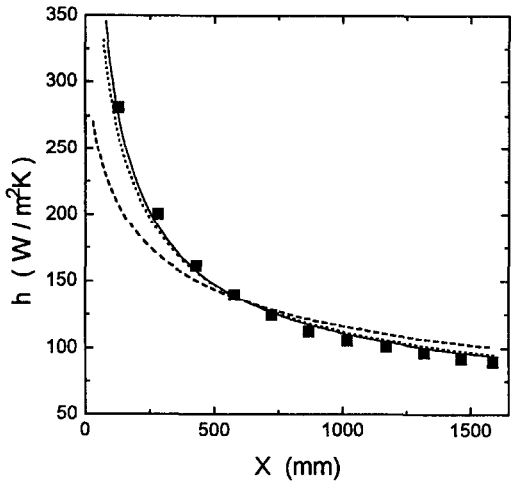

Fig. 9. Comparison between experimental heat transfer coefficients measured by Wu *et al.* [7] on a membrane wall and predictions of the determinate contact distance model with fitted parameters. For solid line $\delta = 0.01$, $R_w = 1/18\,000$ m^2 K W^{-1}, $K = 290$ and $L = 2.86$ m; for dotted line $\delta = 0.1$, $R_w = 1/1800$ m^2 K W^{-1}, $K = 28.2$ and $L = 3.18$ m; for dashed line $\delta = 0.4$, $R_w = 1/450$ m^2 K W^{-1}, $K = 6.34$ and $L = 4.87$ m.

COMPARISON OF MODEL WITH EXPERIMENTAL RESULTS

Few detailed experimental studies on local heat transfer coefficient variation with length are available. The experimental results for a membrane wall reported by Wu *et al.* [7] were chosen to compare with model prediction. For this purpose the determinate contact distance model presented above is employed due to its simplicity. At this stage radiative heat transfer is assumed negligible for the bed temperature of 407°C. The average cluster voidage and the fraction of wall covered by clusters were evaluated according to relationships suggested by Lints and Glicksman [11]. Non-linear least square fitting was then used to evaluate the dimensionless parameter K as well as the wall contact resistance R_w and mean cluster contact distance L. From these results the product $k_e \rho c u$ can also be estimated from the definition of K, equation (13).

The interface contact resistance R_w is commonly expressed in terms of the width, δd_p, of a gas gap required to give the same resistance, i.e.

$$R_w = \frac{\delta d_p}{k_g}. \tag{28}$$

Theoretically, R_w can be fitted directly to experimental data. However, the fitting led to a very small R_w value ($\delta < 0.01$) relative to previous work in bubbling and circulating beds, where $0.1 \leqslant \delta \leqslant 0.4$. Fitting results with $\delta = 0.4$, 0.1 and 0.01 are shown in Fig. 9. Although the fit with $\delta = 0.01$ (solid line) gave the best fit, the fit is still reasonable with $\delta = 0.1$, a value often used for bubbling fluidized beds. Some researchers [9,11] have suggested a larger contact resistance for CFB on the basis of experimental measurements with δ being around 0.4. However, $\delta = 0.4$ (dashed line) gave a less satisfactory fit here.

The computed average cluster convective transfer coefficient for a small (10 mm long) probe can be less than 45% of $1/R_w$, with R_w fitted as above ($\delta = 0.1$). The greater the K, i.e. the smaller the R_w, the sharper the drop in the heat transfer coefficient for the initial section of the surface, as shown in Fig. 8. This may have caused overestimation of R_w in some experiments. An improved fit was evident for most values of R_w when the first data point ($x = 130$ mm) was excluded. This may be because of extra heat absorption by the inlet pipe and/or disturbance at the junction between the top of the membrane wall and the refractory above in the experimental layout. The values of u, the particle velocity of descent at the wall, which correspond to the fitted values of K and L, are 1.07, 0.57 and 0.48 m s^{-1} for $\delta = 0.4$, 0.1 and 0.01, respectively. These values are close to the range of values determined experimentally, which typically range from about 1 to 1.8 m s^{-1} [12].

There are very few data available which could permit mean cluster contact distances to be derived. The model presented above provides a feasible approach to this problem through measuring heat transfer coefficient variation with length. The fitting for the membrane wall data suggests a mean contact distance in excess of 3 m. Such long lengths could be explained by the shielding effect of membrane walls, which hinders renewal of clusters sliding downwards along the fins [2]. When more experimental data are available for both smooth and membrane walls, the information on the mean cluster contact distance can be used to study the influence of the wall geometry on hydrodynamics in the wall vicinity.

CONCLUDING REMARKS

Particle convective heat transfer in circulating fluidized beds occurs due to solid streamers, which, according to their thermal history, have different temperatures on their contact interfaces and, hence, different transfer potentials. While previous models tracing the thermal history of the clusters have provided a basis for this kind of heat transfer calculation, they have failed to provide accurate insight into the local transfer rate. The 'local' models presented here are based on the weighted average of contributions of various clusters; a clear link between the 'transient' models and 'local' models has been derived. Both local and area-averaged particle convective heat transfer on surfaces of all lengths can then be predicted. The model which assumes that cluster contact distances conform to a certain probabilistic distribution depicts cluster heat transfer more realistically than previous models. While the magnitude and dependence of the contact distance variance remain to be investigated, computer simulation has indicated that this variance is of such minor significance that the heat transfer coefficients vary within only 7% as the parameter n varies over a vast range from 2 to infinity. This indicates that it is the mean of the cluster contact distances rather than their distribution that primarily determines the particle convective heat transfer. The simplified determinate contact distance model, which ignores the contact distance distribution, is therefore usually adequate for practical purposes. Explicit functional relations for both local and area-averaged heat transfer coefficients can be derived from this simplified model.

Measurements of local or average heat transfer coefficients along heat transfer surfaces can be used to estimate unknown parameters R_w and L in the model. Here the model was fitted to experimental results for a membrane wall. Further tests and study are needed to obtain a better understanding of the cluster renewal and its influence on heat transfer, as well as to make allowance for combined conductive and radiative heat transfer at higher temperatures.

REFERENCES

1. J. R. Grace, Heat transfer in circulating fluidized beds. In *Circulating Fluidized Bed Technology* (Edited by P. Basu), pp. 63–80. Pergamon Press, Toronto (1986).
2. J. R. Grace, Heat transfer in high velocity fluidized beds, *Proceedings of the Ninth International Heat Transfer Conference*, pp. 329–339. Jerusalem (1990).
3. S. H. Mickley and D. F. Fairbanks, Mechanism of heat transfer to fluidized beds, *A.I.Ch.E. Jl* **1**, 1135–1147 (1955).
4. A. P. Baskakov, The mechanism of heat transfer between a fluidized bed and a surface, *Int. Chem. Engng* **4**, 320–324 (1964).
5. N. I. Gelperin and V. G. Einstein, Heat transfer in fluidized beds. In *Fluidization* (Edited by J. F. Davidson and D. Harrison), pp. 471–538. Academic Press, London (1971).
6. A. H. George, Instantaneous local heat transfer coefficients and related frequency spectra for a horizontal cylinder in a high temperature fluidized bed, *Int. J. Heat Mass Transfer* **36**, 337–345 (1993).
7. R. L. Wu, J. R. Grace, C. J. Lim and C. Brereton, Suspension-to-surface heat transfer in a circulating fluidized bed combustor, *A.I.Ch.E. Jl* **35**, 1685–1691 (1989).
8. L. R. Glicksman, Circulating fluidized bed heat transfer. In *Circulating Fluidized Bed Technology* II (Edited by P. Basu and J. F. Large), pp. 13–29. Pergamon Press, Toronto (1988).
9. R. L. Wu, J. R. Grace and C. J. Lim, A model for heat transfer in circulating fluidized beds, *Chem. Engng Sci.* **45**, 3389–3398 (1990).
10. P. Basu, Heat transfer in high temperature fast fluidized beds, *Chem. Engng Sci.* **45**, 3123–3136 (1990).
11. M. C. Lints and L. R. Glicksman, Parameters governing particle-to-wall heat transfer in a circulating fluidized bed. In *Circulating Fluidized Bed Technology* IV (Edited by A. A. Avidan), pp. 297–304. A.I.Ch.E., New York (1993).
12. R. L. Wu, C. J. Lim, J. R. Grace and C. M. H. Brereton, Instantaneous local heat transfer and hydrodynamics in a circulating fluidized bed, *Int. J. Heat Mass Transfer* **34**, 2019–2027 (1991).